

# Bifurcation analysis of the twist-Fréedericksz transition in a nematic liquid-crystal cell with pre-twist boundary conditions

FERNANDO P. DA COSTA<sup>1</sup>, EUGENE C. GARTLAND, JR.<sup>2</sup>,  
MICHAEL GRINFELD<sup>3</sup> and JOÃO T. PINTO<sup>4</sup>

<sup>1</sup>*Departamento de Ciências e Tecnologia, Universidade Aberta, Rua Fernão Lopes, 9, 2º Dto., P-1000-132 Lisboa, Portugal, and Centro de Análise Matemática, Geometria e Sistemas Dinâmicos, Instituto Superior Técnico, TU Lisbon, Av. Rovisco Pais, 1, P-1049-001 Lisboa, Portugal*

*email: fcosta@univ-ab.pt*

<sup>2</sup>*Department of Mathematical Sciences, Kent State University, P.O. Box 5190, Kent, OH 44242-0001, USA*

*email: gartland@math.kent.edu*

<sup>3</sup>*Department of Mathematics, University of Strathclyde, 26 Richmond Street, Glasgow G1 1XH, UK*

*email: caas05@maths.strath.ac.uk*

<sup>4</sup>*Department of Mathematics and Centro de Análise Matemática, Geometria e Sistemas Dinâmicos, Instituto Superior Técnico, TU Lisbon, Av. Rovisco Pais, 1, P-1049-001 Lisboa, Portugal*

*email: jpinto@math.ist.utl.pt*

(Received 8 July 2008; revised 11 January 2009; first published online 16 February 2009)

Motivated by a recent investigation of Millar and McKay [Director orientation of a twisted nematic under the influence of an in-plane magnetic field. *Mol. Cryst. Liq. Cryst* **435**, 277/[937]–286/[946] (2005)], we study the magnetic field twist-Fréedericksz transition for a nematic liquid crystal of positive diamagnetic anisotropy with strong anchoring and pre-twist boundary conditions. Despite the pre-twist, the system still possesses  $\mathbb{Z}_2$  symmetry and a symmetry-breaking pitchfork bifurcation, which occurs at a critical magnetic-field strength that, as we prove, is above the threshold for the classical twist-Fréedericksz transition (which has no pre-twist). It was observed numerically by Millar and McKay that this instability occurs precisely at the point at which the ground-state solution loses its monotonicity (with respect to the position coordinate across the cell gap). We explain this surprising observation using a rigorous phase-space analysis.

## 1 Introduction

Liquid crystals are materials that exhibit partially ordered fluid phases under certain conditions (usually dependent on temperature or relative concentration, in the case of mixtures). The simplest liquid-crystal phase is the *nematic*, which possesses orientational order but no positional order. This phase is often associated with long rod-like molecules, and the orientational order is typically modelled by a unit length vector field, the *director field*, which represents the average orientation of the long axes of the molecules in a volume element at a point. Standard references on liquid crystals include Chandrasekhar

[2], de Gennes and Prost [5] (for the physics of liquid crystals), Stewart [12] and Virga [13] (from the point of view of applied mathematics).

The configuration of the director field in a confined system is influenced by several factors, including the intrinsic elasticity of the material (the preference of the molecules to orient themselves parallel to each other), externally applied electric or magnetic fields (which can encourage the director to align either parallel to the field or perpendicular to it, depending on the material), boundary conditions imposed by confining substrates, and viscous torques arising from fluid flow. The local orientation of the director influences the stress tensors that govern the fluid velocity variables. A full, coupled, macroscopic model of the hydrodynamics of a liquid crystal (valid in certain parameter regimes) is given by the *Ericksen–Leslie equations*, which contain the *Oseen–Frank elastic theory* governing the steady state, equilibrium solutions.

In some systems, the coupling between director re-orientation and fluid flow can be neglected (to leading order). The simplest model for the dissipative dynamics of the director field in the absence of flow can be expressed as a gradient flow of the *free energy* of the system and takes the general form:

$$\gamma_1 \frac{\partial \mathbf{n}}{\partial \tau} = \operatorname{div} \left( \frac{\partial w}{\partial \nabla \mathbf{n}} \right) - \frac{\partial w}{\partial \mathbf{n}} - \lambda \mathbf{n},$$

or, in terms of components,

$$\gamma_1 \frac{\partial n_\alpha}{\partial \tau} = \frac{\partial}{\partial x_\beta} \left( \frac{\partial w}{\partial n_{\alpha,\beta}} \right) - \frac{\partial w}{\partial n_\alpha} - \lambda n_\alpha,$$

where  $n_{\alpha,\beta} := \frac{\partial n_\alpha}{\partial x_\beta}$ . Here  $\gamma_1$  is a single rotational viscosity,  $\mathbf{n}$  is the director field,  $\tau$  is time,  $w$  is the free-energy density,  $\lambda$  is a Lagrange-multiplier field to enforce the pointwise unit-vector constraint  $|\mathbf{n}| = 1$ , and summation over repeated indices is implied in the component form. For a system with strong anchoring, occupying a region  $\Omega$ , and in the presence of a magnetic field, an appropriate form for the total free energy of a given director field,

$$\int_{\Omega} w(\mathbf{n}, \nabla \mathbf{n}),$$

is provided by the free-energy density:

$$2w = K_1 (\operatorname{div} \mathbf{n})^2 + K_2 (\mathbf{n} \cdot \operatorname{curl} \mathbf{n})^2 + K_3 |\mathbf{n} \times \operatorname{curl} \mathbf{n}|^2 - \mu_0 \Delta \chi (\mathbf{H} \cdot \mathbf{n})^2,$$

where  $K_1$ ,  $K_2$  and  $K_3$  are phenomenological elastic constants,  $\mu_0$  is the free-space magnetic permeability,  $\Delta \chi = \chi_{\parallel} - \chi_{\perp}$  is the difference between the diamagnetic susceptibilities parallel to versus perpendicular to the director and  $\mathbf{H}$  is the magnetic field (assumed to be constant in  $\Omega$ ). The free-energy density embodies the competition between the energy cost of distortions of the director field versus the energy reduction associated with aligning parallel to the magnetic field (if  $\Delta \chi$  is positive). For example, see [12].

A common geometry for liquid-crystal devices and experiments is that of a thin film, with the confining substrates treated to coerce a particular orientation of the director. Under the influence of a sufficiently strong electric or magnetic field, the equilibrium ground state of the director field (which is typically uniform and undistorted) becomes unstable

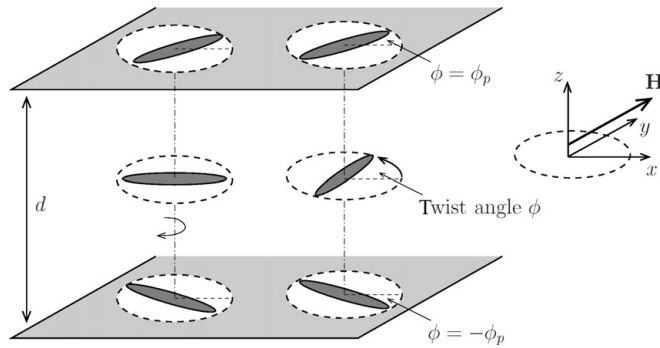


FIGURE 1. Geometry of the liquid-crystal cell.

to a solution more aligned with the applied field. This is called a *Fréedericksz transition*. It is the most basic and fundamental instability in liquid crystals and is discussed in all of the standard references on the subject. From a practical point of view, such transitions can be used in experiments to determine values for the elastic constants of different materials. Also, it is typically the case that the equilibrium director fields on either side of a Fréedericksz threshold give the ‘on’ and ‘off’ states for various liquid-crystal devices.

We consider the geometry of the twist-Fréedericksz transition, with an antisymmetric pre-twist. Thus we consider a slab of nematic material bounded by two parallel planes a distance  $d$  apart from each other, unbounded and extending to infinity in any direction parallel to these planes. Define a positively oriented orthogonal coordinate system  $(x, y, z)$  such that  $z$  is perpendicular to the bounding planes. Let the director field be represented by

$$\mathbf{n} = (\cos \phi(\tau, z), \sin \phi(\tau, z), 0), \quad (1.1)$$

where  $\phi$  denotes the (twist) angle of the director. We will assume that in the liquid-crystal cell the director is fixed in opposing orientations  $-\phi_p$  and  $\phi_p$  at the two opposing planes bounding the device in the  $z$  direction. This induces a net twist of the director vector field across the cell (see Figure 1). We will consider a magnetic vector field  $\mathbf{H}$  applied along the constant direction  $(0, 1, 0)$  with varying intensity  $H = \|\mathbf{H}\|$  and are interested in studying the effect it induces in the stationary director distribution, according to Ericksen–Leslie theory.

The angle representation (1.1) guarantees satisfaction at all points and times of the unit-vector constraint  $|\mathbf{n}| = 1$ . In terms of this representation, the free-energy density and director dynamics equation become

$$2w(\phi, \phi_z) = K_2 \phi_z^2 - \mu_0 \Delta \chi H^2 \sin^2 \phi, \quad \phi_z := \frac{\partial \phi}{\partial z},$$

and

$$\gamma_1 \frac{\partial \phi}{\partial \tau} = \frac{\partial}{\partial z} \left( \frac{\partial w}{\partial \phi_z} \right) - \frac{\partial w}{\partial \phi} = K_2 \frac{\partial^2 \phi}{\partial z^2} + \mu_0 \Delta \chi H^2 \sin \phi \cos \phi.$$

In dimensionless form, the initial-boundary value problem governing the behaviour of the director field is then

$$\frac{\partial \phi}{\partial s} = \frac{\partial^2 \phi}{\partial \zeta^2} + \lambda \sin \phi \cos \phi, \quad (s, \zeta) \in \mathbb{R}^+ \times (0, 1), \tag{1.2}$$

$$\phi(\cdot, 0) = -\phi_p, \quad \phi(\cdot, 1) = \phi_p, \tag{1.3}$$

$$\phi(0, \cdot) = \phi_0, \tag{1.4}$$

where

$$s := \frac{K_2}{\gamma_1 d^2} \tau, \quad \zeta := \frac{z}{d}, \quad \lambda := \frac{\mu_0 \Delta \chi H^2 d^2}{K_2}. \tag{1.5}$$

All the material parameters are positive for our system of interest. Observe that the dimensionless control parameter  $\lambda$  is proportional to the square of the magnetic field strength.

The associated equilibrium problem is given by

$$\frac{d^2 \phi}{d\zeta^2} + \lambda \sin \phi \cos \phi = 0, \quad 0 < \zeta < 1, \tag{1.6}$$

$$\phi(0) = -\phi_p, \quad \phi(1) = \phi_p. \tag{1.7}$$

In the classical twist-Fréedericksz transition problem, we have  $\phi_p = 0$ ; the system possesses a simple mirror symmetry,  $\phi(\zeta) \leftrightarrow -\phi(\zeta)$ ; and the ground-state solution ( $\phi = 0$ , which is invariant under this symmetry) loses stability to a pair of mirror-symmetric, distorted solutions at a pitchfork bifurcation at the critical threshold value  $\lambda_c$  of the parameter  $\lambda = \lambda(\phi_p)$  given by,

$$\lambda_c := \lambda_c(0) = \pi^2 \Leftrightarrow H_c := \frac{\pi}{d} \sqrt{\frac{K_2}{\mu_0 \Delta \chi}}.$$

In a system with pre-twist ( $\phi_p \neq 0$ ), we no longer have the simple reflection symmetry above. The problem still possesses  $\mathbb{Z}_2$  symmetry, however, it is now of the form  $\phi(\zeta) \leftrightarrow -\phi(1 - \zeta)$ . The ground-state solution (which is invariant under this symmetry) is no longer uniform, but undergoes a net twist from  $\zeta = 0$  to  $\zeta = 1$ . For  $\lambda = 0$ , it is simply the linear profile  $\phi(\zeta) = (2\zeta - 1)\phi_p$ . The problem still has a classical pitchfork bifurcation diagram, with the symmetric solution branch bifurcating at a value  $\lambda_c(\phi_p)$ , which is necessarily greater than  $\pi^2$ , as we show below, to a pair of symmetry-related non-symmetric solutions. We note that the antisymmetric nature of the boundary conditions is crucial to this scenario.

This system was carefully studied numerically by Millar and McKay in [8, 9]. They found that the ground-state solution is a strictly monotone increasing function of  $\zeta$  for  $0 \leq \lambda \leq \lambda_c(\phi_p)$ . At  $\lambda = \lambda_c(\phi_p)$ , this solution satisfies homogeneous Neumann boundary conditions  $\phi'(0) = \phi'(1) = 0$ , in addition to the Dirichlet ('strong anchoring') conditions  $\phi(0) = -\phi_p$  and  $\phi(1) = \phi_p$ . For  $\lambda > \lambda_c(\phi_p)$ , this solution is no longer monotone and possesses a unique interior minimum and maximum (see Figure 2). Thus, Millar and McKay observed the surprising fact that the symmetry-breaking bifurcation coincided with the loss of monotonicity of the ground-state solution. Here we shall use a rigorous phase-plane analysis to explain this fact.

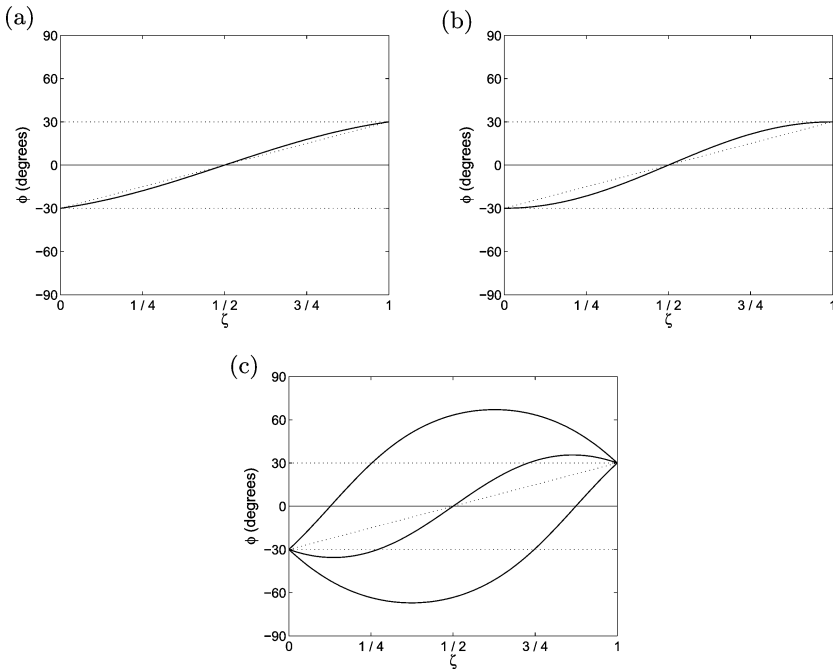


FIGURE 2. Twist-angle profiles of the symmetric ground-state solution with  $\phi_p = \frac{\pi}{6}$  and for (a)  $\lambda = \frac{1}{2}\lambda_c(\phi_p)$ , (b)  $\lambda = \lambda_c(\phi_p)$  and (c)  $\lambda = 2\lambda_c(\phi_p)$ , and the concomitant loss of symmetry and monotonicity and simultaneous satisfaction of both Dirichlet and homogeneous Neumann boundary conditions at  $\lambda = \lambda_c(\phi_p)$ .

### 2 Time maps

In this section, we shall be concerned only with the stationary solutions to (1.2)–(1.4), i.e. with the solutions of (1.6)–(1.7). Consider the change of variables  $t = t(\zeta) := \sqrt{\frac{\lambda}{2}}(\zeta - \frac{1}{2})$ , and let  $\zeta(t)$  be its inverse function. Let

$$L := \sqrt{\frac{\lambda}{8}}. \tag{2.1}$$

Then,  $\phi(\zeta)$  is a solution of (1.6)–(1.7) if and only if  $x(t) := \phi(\zeta(t))$  is a solution of

$$\begin{cases} x' = y \\ y' = -\sin 2x \end{cases}, \tag{2.2}$$

$$x(-L) = -\phi_p, \quad x(L) = \phi_p. \tag{2.3}$$

The bifurcation parameter is now  $L$ . Note that  $L \propto H$ . We shall treat the independent variable  $t$  in (2.2)–(2.3) as the ‘time’ of the dynamical system associated with (2.3). Note that this ‘time’ corresponds to the original spacial variable  $\zeta$  and not to the original time  $s$ .

Let us start by observing that (2.2) is a nonlinear pendulum equation with first integral,

$$V(x, y) = y^2 - \cos 2x, \tag{2.4}$$

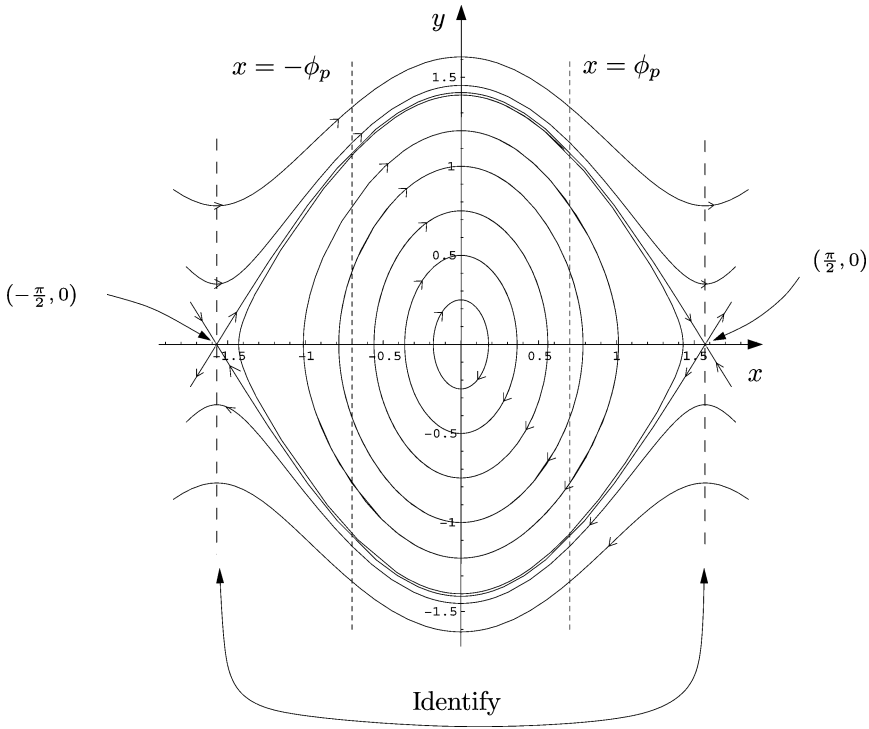


FIGURE 3. Orbits of (2.2) with the boundary conditions (2.3).

and thus its orbits are contained in the level sets of  $V$ . The natural phase space for (2.2)–(2.3) is the strip  $[-\frac{\pi}{2}, \frac{\pi}{2}] \times \mathbb{R}$  with the straight lines  $x = -\frac{\pi}{2}$  and  $x = \frac{\pi}{2}$  identified; which is, obviously, the same as a cylindrical phase space (Figure 3). We shall use either interpretation (as a strip or as a cylinder) as appropriate.

Observing that, for all  $\alpha \in (0, \frac{\pi}{2})$ , the orbit  $\gamma_\alpha$  that intersects the  $x$ -axis at  $(\alpha, 0)$  is periodic, we can associate to each of these values of  $\alpha$  the quantity  $T(\alpha) = \frac{1}{4}P(\alpha)$ , where  $P(\alpha)$  is the period of the corresponding orbit  $\gamma_\alpha$ . By the symmetry properties of (2.2)–(2.3) under the transformations  $x \mapsto -x$  and  $y \mapsto -y$ , we conclude that  $T(\alpha)$  is the time needed for the point of intersection of  $\gamma_\alpha$  with the positive- $y$  semi-axis,  $(0, \sqrt{2} \sin \alpha)$ , to travel to  $(\alpha, 0)$ . Using (2.2) in (2.4) we get,

$$T(\alpha) := \int_0^\alpha \frac{dx}{\sqrt{\cos 2x - \cos 2\alpha}}. \tag{2.5}$$

We will also need the time map  $(\alpha, \phi_p) \mapsto T_1(\alpha, \phi_p)$  measuring the time needed for the point of intersection of the orbit  $\gamma_\alpha$  with the positive- $y$  semi-axis to travel to the straight line  $x = \phi_p \leq \alpha$ , corresponding to the boundary condition (2.3):

$$T_1(\alpha, \phi_p) := \int_0^{\phi_p} \frac{dx}{\sqrt{\cos 2x - \cos 2\alpha}}. \tag{2.6}$$

Clearly  $T_1(\phi_p, \phi_p) = T(\phi_p)$ .

An analogous time map can be defined for orbits that cross the positive- $y$  semi-axis at a point above the orbit  $\gamma_h$  joining  $(-\frac{\pi}{2}, 0)$  to  $(\frac{\pi}{2}, 0)$  (note that  $\gamma_h$  is a heteroclinic orbit if we do not identify its endpoints as a single point, or a homoclinic orbit when we consider the cylindrical picture of the phase space). Using the first integral (2.4) we easily conclude that  $\gamma_h$  crosses the positive- $y$  semi-axis at the point  $(0, \sqrt{2})$ . For every  $\beta \geq \sqrt{2}$  and  $\phi_p \in (0, \frac{\pi}{2})$  the time map  $(\beta, \phi_p) \mapsto T_2(\beta, \phi_p)$  defined by

$$T_2(\beta, \phi_p) := \int_0^{\phi_p} \frac{dx}{\sqrt{\beta^2 + \cos 2x - 1}}, \tag{2.7}$$

measures the time taken by the point  $(0, \beta)$  to reach the line  $x = \phi_p$  under the flow generated by (2.2). By the dominated convergence theorem, we have  $T_2(\beta, \phi_p) \rightarrow 0$  as  $\beta \rightarrow +\infty$ .

The time map  $T_2$  can be used to compute the periods of the periodic orbits above  $\gamma_h$ : if the orbit crosses the positive- $y$  semi-axis at a point  $(0, \beta)$  with  $\beta > \sqrt{2}$ , its period is  $2T_2(\beta, \frac{\pi}{2})$ . Observe that, by the symmetry of (2.2) under the transformations  $x \mapsto -x$  and  $y \mapsto -y$ , the orbits crossing the negative- $y$  semi-axis at a point  $(0, -\beta)$  below the orbit  $\gamma_{-h}$  connecting  $(\frac{\pi}{2}, 0)$  to  $(-\frac{\pi}{2}, 0)$ , have a period given by the same expression.

The function  $T_2$  can be continuously extended for values  $\beta < \sqrt{2}$  using the time map  $T_1$ : by the phase portrait presented in Figure 3 and the fact that orbits of (2.2) lie on level sets of the first integral  $V$ , we conclude that, for each  $\alpha \in (0, \frac{\pi}{2})$ , there exists a unique  $\beta = \beta(\alpha) \in (0, \sqrt{2})$  such that the points  $(0, \beta)$  and  $(\alpha, 0)$  lie on the same orbit of (2.2), and the function  $\alpha \mapsto \beta(\alpha)$  is strictly increasing. Thus, denoting by  $\beta^*$  the value of  $\beta(\phi_p)$ , we conclude that, for each  $\alpha \in [\phi_p, \frac{\pi}{2})$ , we have  $\beta(\alpha) \in [\beta^*, \sqrt{2})$ . Denoting by  $\beta \mapsto \alpha(\beta)$  the inverse function, we can extend the definition of  $T_2$  to  $\beta \in [\beta^*, \sqrt{2})$  as follows:

$$T_2(\beta, \phi_p) := T_1(\alpha(\beta), \phi_p). \tag{2.8}$$

Observe that the following equalities hold,  $T_2(\beta^*, \phi_p) = T_1(\phi_p, \phi_p) = T(\phi_p) = L^*$ , where, for later reference, we have defined:

$$L^* := T(\phi_p). \tag{2.9}$$

We also observe that, by continuous dependence of the flow generated by (2.2), we have  $\beta^* := \beta(\phi_p) \rightarrow \sqrt{2}$  as  $\phi_p \rightarrow \frac{\pi}{2}$ .

In order to proceed with the analysis we need the following result about the monotonicity properties of the time maps  $T$ ,  $T_1$  and  $T_2$ :

**Proposition 1** *Let  $\alpha \in (0, \frac{\pi}{2})$ ,  $\phi_p \in (0, \alpha)$ , and  $\beta \geq \beta^*$ . Then,*

- (1) *the function  $\alpha \mapsto T(\alpha)$  defined by (2.5) is strictly increasing and converges to  $+\infty$  as  $\alpha \uparrow \frac{\pi}{2}$ , and to  $\frac{\pi}{2\sqrt{2}}$  as  $\alpha \downarrow 0$ .*
- (2) *the functions  $\alpha \mapsto T_1(\alpha, \phi_p)$  and  $\beta \mapsto T_2(\beta, \phi_p)$ , defined by (2.6) and (2.7), respectively, are strictly decreasing. The same holds true for  $T_2(\cdot, \frac{\pi}{2})$ .*

**Proof 1** As in [11], we change the integration variable  $x \mapsto s := \frac{x}{\alpha}$  in (2.5), so that

$$T(\alpha) = \int_0^1 \frac{\alpha}{\sqrt{\cos 2\alpha s - \cos 2\alpha}} ds,$$

and thus

$$T'(\alpha) = \int_0^1 \frac{\theta(\alpha s) - \theta(\alpha)}{(\cos 2\alpha s - \cos 2\alpha)^{3/2}} ds, \tag{2.10}$$

where  $\theta(x) := \cos 2x + x \sin 2x$ . Since  $\theta$  is strictly decreasing in  $(0, \frac{\pi}{2})$ , we conclude that the integrated function in (2.10) is positive and thus  $T(\cdot)$  is strictly increasing. The limit behaviours are readily obtained from the facts that the orbits approach  $\gamma_h$  in the first case, and the flow becomes close to the linearized flow about  $(0, 0)$  in the second case.

**Proof 2** Differentiating  $T_1$  with respect to  $\alpha$ , we get,

$$\frac{\partial T_1}{\partial \alpha} = - \int_0^{\phi_p} \frac{\sin 2x}{(\cos 2x - \cos 2\alpha)^{3/2}} dx < 0. \tag{2.11}$$

For  $\beta > \sqrt{2}$  we use (2.7) to get

$$\frac{\partial T_2}{\partial \beta} = - \int_0^{\phi_p} \frac{\beta}{(\beta^2 + \cos 2x - 1)^{3/2}} dx < 0,$$

which is valid for all  $\phi_p \in (0, \frac{\pi}{2}]$ . With  $\beta \in (\beta^*, \sqrt{2})$ , using (2.8), the fact that  $\beta \mapsto \alpha(\beta)$  is strictly increasing, and the above computation of  $\frac{\partial T_1}{\partial \alpha}$ , we conclude that

$$\frac{\partial T_2}{\partial \beta} = \frac{\partial T_1}{\partial \alpha} \frac{d\alpha}{d\beta} < 0.$$

The result now follows from these inequalities and the continuity of  $T_2(\cdot, \phi_p)$  at  $\beta^*$  and  $\sqrt{2}$ . □

### 3 Phase-space analysis

With recourse to the time-maps' properties established in the previous section, we can now start our bifurcation analysis of (2.2)–(2.3). At this point it is important to separate the study of orbits bounded by the homoclinic loops  $\gamma_h$  and  $\gamma_{-h}$ , from those existing in the unbounded regions of the cylindrical phase plane. We will deal with the first ones in Sections 3.1–3.3 and with the last ones in Section 3.4.

For the study of the orbits in the bounded region we can consider the system as living in the strip  $(-\frac{\pi}{2}, \frac{\pi}{2}) \times \mathbb{R}$  of  $\mathbb{R}^2$ . Naturally, for the study of the solutions in the unbounded regions the consideration of the cylindrical nature of the phase plane is mandatory. For all Sections 3.1–3.3 below, remember that we have defined  $L^*$ , in (2.9), as the value of  $T(\cdot)$  at  $\phi_p$ .



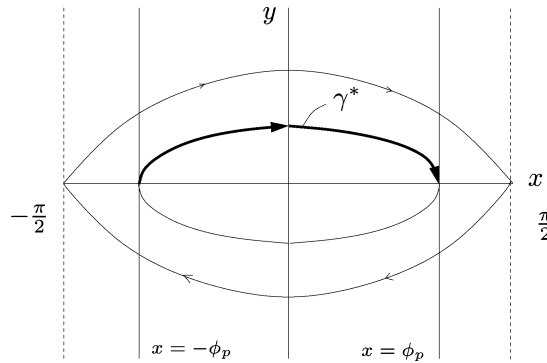


FIGURE 4. The orbit  $\gamma_*$  of the solution  $(x^*, y^*)$  of (2.2)–(2.3) when  $L$  is the critical value  $L^*$ .

### 3.1 The critical case $L = L^*$

A first and easy consequence of last section’s results is that, for every  $\phi_p \in (0, \pi/2)$ , there exists a unique solution  $(x^*, y^*)$ , to the boundary value problem (2.2)–(2.3) with  $L = L^*$ . In fact, if we fix  $\phi_p \in (0, \pi/2)$ , the monotone increasing behaviour of  $T(\cdot)$  given by Proposition 1 implies that there exists a unique value of  $\alpha$ , namely  $\phi_p$ , such that  $T(\alpha) = L^*$ . Observe that the  $x$ -component of this unique solution is strictly increasing and satisfies both Dirichlet and homogeneous Neumann boundary conditions (Figure 4).

### 3.2 The subcritical case $L < L^*$

Another equally easy consequence of the monotonicity of the time maps is that, for each fixed value of  $\phi_p \in (0, \pi/2)$  and each  $L \in (0, L^*)$ , there exists one and only one solution to (2.2)–(2.3). Furthermore, all these solutions have a monotone increasing  $x$ -component.

To establish this, let us start by fixing  $\phi_p \in (0, \pi/2)$ . For this  $\phi_p$ , compute  $L^*$  by (2.9) and choose an arbitrary  $L \in (0, L^*)$ . From the definition and properties of  $T_2$  in Section 2, we conclude that there exists a unique  $\beta_L > \beta^*$  such that  $T_2(\beta_L, \phi_p) = L$ .

Consider the orbit  $\gamma_{\beta_L}$  of (2.2) that contains the point  $(0, \beta_L)$ . By construction, the arc of  $\gamma_{\beta_L}$  between the lines  $x = -\phi_p$  and  $x = \phi_p$  satisfies the boundary condition (2.3). By the monotonicity of  $T_2$  it follows that  $L \mapsto \beta_L$  is strictly decreasing, and the uniqueness of  $\beta_L$  implies the uniqueness of the solution to (2.2)–(2.3). The monotonicity of the  $x$ -component of the solution as a function of  $t$  is obvious from the phase portrait in Figure 3.

### 3.3 The supercritical case $L > L^*$

Finally, again using the monotonicity of the time maps, we can establish the existence, for all  $L > L^*$ , of several branches of solutions, three of them bifurcating from the critical solution  $(x^*, y^*)$  at  $L = L^*$ .

#### 3.3.1 Asymmetric solutions bifurcating from $\gamma_*$

Fix any  $L > L^*$ . By Proposition 1, there exists a unique  $\alpha = \alpha(L) \in (\phi_p, \frac{\pi}{2})$ , such that  $T(\alpha) = L$ . Hence, there exists a unique solution of (2.2) satisfying the boundary condition

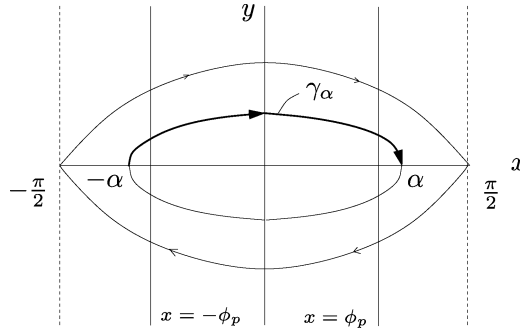


FIGURE 5. The orbit  $\gamma_\alpha$  of (2.2) with period  $4L$ , with  $L > L^*$ , and the arc of  $\gamma_\alpha$  that satisfies the boundary condition  $x(-L) = -\alpha$  and  $x(L) = \alpha$ .

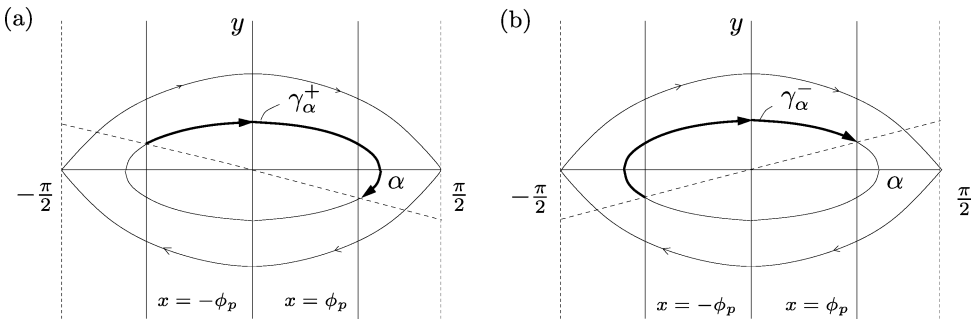


FIGURE 6. The orbits  $\gamma_\alpha^+$  and  $\gamma_\alpha^-$  of (2.2) that satisfy the boundary condition (2.3) where  $\alpha$  is the unique solution of  $T(\alpha) = L$ , for  $L > L^*$ .

$x(-L) = -\alpha$  and  $x(L) = \alpha$  and with strictly increasing  $x$ -component; corresponding to this solution is the arc between the points  $(-\alpha, 0)$  and  $(\alpha, 0)$  of the periodic orbit  $\gamma_\alpha$  of (2.2) plotted in Figure 5.

By construction,  $\gamma_\alpha$  has period  $4L$ , and by the invariance of the vector field of (2.2) under the transformations  $x \mapsto -x$  and  $y \mapsto -y$ , one concludes that, in any one period, the orbit spends exactly  $2L$  units of time in every half-strip. This implies that there exists exactly two solutions of (2.2)–(2.3) whose orbits, denoted by  $\gamma_\alpha^+$  and  $\gamma_\alpha^-$ , coincide with part of  $\gamma_\alpha$  and lie entirely in a half-space, as presented in Figures 6(a) and (b).

It is clear from the limit behaviour of  $T$  at  $\frac{\pi}{2}$  stated in Proposition 1, that the branches of solutions corresponding to the orbits  $\gamma_\alpha^+$  and  $\gamma_\alpha^-$  exist globally as  $L \rightarrow +\infty$  and remain bounded. Clearly, since  $\alpha \downarrow \phi_p$  as  $L \downarrow L^*$ , the two orbits converge to the orbit  $\gamma_*$  of the critical solution  $(x^*, y^*)$  as  $L \rightarrow L^*$ . Note that each of these solutions exhibit a single extremum in the interval  $(-L, L)$ : the solution whose orbit is  $\gamma_\alpha^+$  has a maximum, and the one correspondent to  $\gamma_\alpha^-$  has a minimum. Note that these are the asymmetric solutions presented in Figure 2(c).

### 3.3.2 Symmetric solutions bifurcating from $\gamma_*$

For  $L > L^*$  there is an easily obtained further solution of (2.2)–(2.3) that corresponds to the bifurcating symmetric solution shown in Figure 2(c). To reach this conclusion,

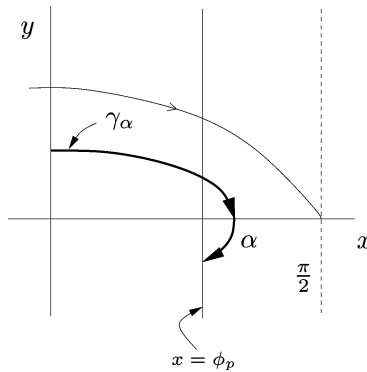


FIGURE 7. The orbit  $\gamma_\alpha$  of (2.2) that satisfies the boundary condition  $x(0) = 0$  and  $x(L) = \phi_p$  referred to in the text.

observe first that the point in the  $y$ -axis of an orbit like the one plotted in Figure 7 takes  $2T(\alpha) - T_1(\alpha, \phi_p)$  units of time to cover its full length.

From Proposition 1,  $T(\cdot)$  and  $T_1(\cdot, \phi_p)$  are both continuous and monotone functions of  $\alpha$  for  $\alpha \in (\phi_p, \frac{\pi}{2})$ , the first one increasing and converging to  $+\infty$  as  $\alpha \rightarrow \frac{\pi}{2}$ , the second one strictly decreasing. Also, remember that  $T(\phi_p) = T_1(\phi_p, \phi_p) = L^*$ . From this it follows that  $2T(\phi_p) - T_1(\phi_p, \phi_p) = L^* < L$  and  $\lim_{\alpha \rightarrow \pi/2} (2T(\alpha) - T_1(\alpha, \phi_p)) = +\infty > L$ . Thus, there exists a unique value of  $\alpha \in (\phi_p, \frac{\pi}{2})$  such that the orbit  $\gamma_\alpha$  plotted in Figure 7 is travelled in  $L$  units of time. Observe that, as  $\alpha \downarrow \phi_p$ , we have  $2T(\alpha) - T_1(\alpha, \phi_p) \rightarrow L^*$  and  $\gamma_\alpha \rightarrow \gamma^*$ . By the symmetry  $x \leftrightarrow -x$ , this construction allows us to conclude that, for each  $L > L^*$ , there is a single solution of (2.2)–(2.3) with exactly one maximum and one minimum in  $(-L, L)$ , and it bifurcates from the critical solution  $(x^*, y^*)$ . This is the symmetric solution in Figure 2(c).

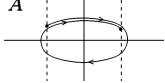
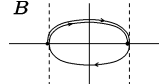
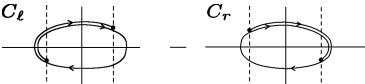
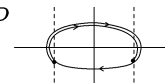
### 3.3.3 Other bifurcating solutions

In this section, we apply the approach used above, based on the interplay of phase-space analysis and the behaviour of the time maps, in order to obtain the existence, at values  $L = L_k^* := (2k + 1)L^*, \forall k \in \mathbb{N}^+$ , of a supercritical pitchfork bifurcation from non-monotonic solutions  $\gamma_{*k}$  whose orbits are akin to  $\gamma_*$  but wind a full  $k$  times around the origin. With this notation,  $\gamma_*$  can be seen as the member  $k = 0$  of this family  $\gamma_{*0}$ , since it does *not* wind around the origin.

We shall also conclude that, for each  $k \in \mathbb{N}^+$ , the branch of symmetric solutions impinging on the pitchfork bifurcation point with  $L < L_k^*$  is one of the branches of solutions arising from a saddle-node point at some  $L_{sn,k} \in [L^*, L_k^*)$ , and no other saddle-node points occur along either of the resulting branches. We start by noting the existence of the five different types of solutions to the boundary value problem (2.2)–(2.3), described in the Table 1 by the letters *A–D*.

Note that, by the same argument used in sections 3.2, 3.3.1 and 3.3.2, all those solutions converge to the critical one  $\gamma_{*k}$  (solution *B*) as  $\alpha \downarrow \phi_p$ , and the time taken by each orbit converges to the corresponding time  $S_B(\phi_p) := 2(2k + 1)T(\phi_p) = 2L_k^*$ . Also by the monotonicity properties of the time maps (Proposition 1), we conclude that, for each fixed

Table 1. Solutions of (2.2)–(2.3), with  $\alpha$  close to  $\phi_p$ , winding  $k$  times around  $\mathbf{0}$ . The symmetry classification of the orbits refers to their behaviour under the reflection  $x \leftrightarrow -x$

$L$	Orbit $\gamma_{\alpha,k}$ (winds $k$ times around $\mathbf{0}$ )	Symmetry of $\gamma_{\alpha,k}$	Time taken by the orbit $\gamma_{\alpha,k}$
$L < L_k^*$		Symmetric	$S_A(\alpha) := 2(2kT(\alpha) + T_1(\alpha, \phi_p))$
$L = L_k^*$		Symmetric	$S_B(\phi_p) := 2(2k + 1)T(\phi_p)$
$L > L_k^*$		Asymmetric	$S_C(\alpha) := 2(2k + 1)T(\alpha)$
$L > L_k^*$		Symmetric	$S_D(\alpha) := 2((2k + 2)T(\alpha) - T_1(\alpha, \phi_p))$

$\alpha > \phi_p$  close to  $\phi_p$ , the time taken by the orbits of type C and D satisfies

$$S_D(\alpha) = S_C(\alpha) + 2(T(\alpha) - T_1(\alpha, \phi_p)) > S_C(\alpha) > S_B(\phi_p) = 2L_k^*,$$

and hence the corresponding branches of solutions occurs supercritically (i.e. at  $L > L_k^*$ ). Analogously, since by (2.10) and (2.11) we have, as  $\alpha \downarrow \phi_p$ ,

$$T'(\alpha) \rightarrow T'(\phi_p) \in (0, \infty), \quad \text{and} \quad \frac{\partial T_1}{\partial \alpha} \rightarrow -\infty, \tag{3.1}$$

the time spent by orbits of type A (with  $\alpha$  sufficiently close to  $\phi_p$ ) satisfy

$$S_A(\alpha) = 2((2k + 1)T(\alpha) + T_1(\alpha, \phi_p) - T(\alpha)) < 2L_k^*,$$

and thus the corresponding branch of solutions occur subcritically (i.e. at  $L < L_k^*$ ). Hence, this concludes the existence of the pitchfork bifurcations alluded to above.

One clear problem arising from the above bifurcation result is that, by the results in Section 3.2, the branch of solutions of type A cannot continue for values of  $L$  below  $L_k^*$ . To understand what happens to these solutions, we study the map  $\alpha \mapsto S_A(\alpha)$ , where  $S_A(\cdot)$  is the time spent by the orbits of type A. For this study, it turns out to be much easier to consider the parametrization of the orbits by  $\tilde{\alpha} := \sin^2 \alpha$  instead of  $\alpha$ . Denote by  $\tilde{S}_A(\tilde{\alpha})$ ,  $\tilde{T}(\tilde{\alpha})$  and  $\tilde{T}_1(\tilde{\alpha})$  the functions  $S_A$ ,  $T$  and  $T_1$  in the new variable. By the definition of  $T$  in (2.5), we can write:

$$T(\alpha) = \tilde{T}(\tilde{\alpha}) = \frac{1}{\sqrt{2}} \int_0^{\frac{\pi}{2}} \frac{d\theta}{\sqrt{1 - \tilde{\alpha} \sin^2 \theta}} = \frac{1}{\sqrt{2}} K(\tilde{\alpha}),$$

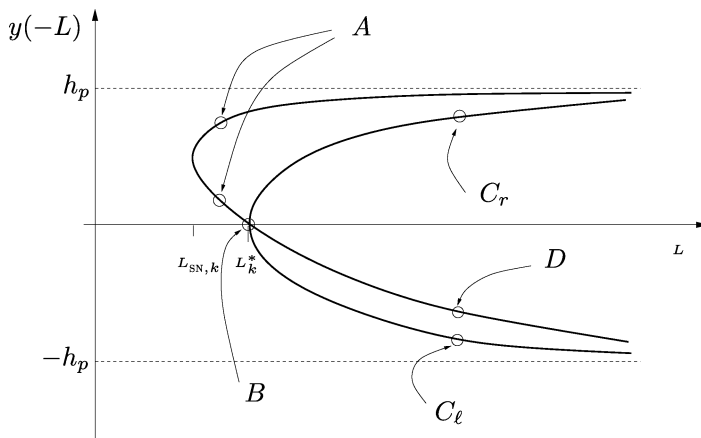


FIGURE 8. Supercritical pitchfork bifurcation diagram around  $L = L_k^*$  where two branches of asymmetric solutions ( $C_r$  and  $C_l$ ) bifurcate from the (symmetric) critical solution  $B$  of (2.2)–(2.3) when  $L$  is the critical value  $L_k^*$ . The symmetric branch ( $A$ ) with  $L < L_k^*$  disappears in a saddle-node bifurcation at  $L = L_{sn,k} \in [L^*, L_k^*)$ . We denote by  $h_p$  (resp.  $-h_p$ ) the value of the  $y$ -component of the orbit  $\gamma_h$  (resp.  $\gamma_{-h}$ ) at the point of intersection with  $x = -\phi_p$ . See Table 1 and the text for further details.

where  $K$  is the complete elliptic integral of the first kind [1, Chapter 17]. From (2.6) we have

$$T_1(\alpha, \phi_p) = \tilde{T}_1(\tilde{\alpha}, \phi_p) = \frac{1}{\sqrt{2}} \int_0^{\phi_p} \frac{dx}{\sqrt{\tilde{\alpha} - \sin^2 x}}.$$

Thus, we have

$$\begin{aligned} \tilde{S}_A''(\tilde{\alpha}) &= 4k\tilde{T}''(\tilde{\alpha}) + 2 \frac{\partial^2 \tilde{T}_1(\tilde{\alpha}, \phi_p)}{\partial \tilde{\alpha}^2} \\ &= \frac{3k}{\sqrt{2}} \int_0^{\frac{\pi}{2}} \frac{\sin^4 \theta}{(1 - \tilde{\alpha} \sin^2 \theta)^{5/2}} d\theta + \frac{3}{2\sqrt{2}} \int_0^{\phi_p} \frac{dx}{(\tilde{\alpha} - \sin^2 x)^{5/2}} > 0. \end{aligned}$$

From Proposition 1 we infer that  $\tilde{S}_A(\tilde{\alpha}) \rightarrow \infty$  as  $\tilde{\alpha} \rightarrow 1$ , and from (3.1) we conclude that  $\tilde{S}_A'(\tilde{\alpha}) \rightarrow -\infty$  as  $\tilde{\alpha} \downarrow \sin^2 \phi_p$ . These arguments, together with the above convexity result, allow us to conclude that the function  $\tilde{\alpha} \mapsto \tilde{S}_A(\tilde{\alpha})$  has a unique minimum for some  $\tilde{\alpha}_{sn,k} \in (\sin^2 \phi_p, 1)$ . We denote by  $L_{sn,k}$  the corresponding minimum value of  $\frac{1}{2}\tilde{S}_A$  (the saddle-node bifurcation point). For all  $L \in (L_{sn,k}, L_k^*)$  there exist exactly two branches of solutions of type  $A$ . Recalling that  $\alpha = \arcsin \sqrt{\tilde{\alpha}}$ , the branch corresponding to the smaller value of  $\alpha$  for fixed  $L$  converges to the critical orbit  $\gamma_{*k}$  (solution  $B$ ) when  $L \uparrow L_k^*$ , while the one corresponding to larger values of  $\alpha$  is defined for all  $L > L_k^*$  and converges to the union of the loops  $\overline{\gamma_h \cup \gamma_{-h}}$ , as  $L \rightarrow +\infty$ . The same monotonicity and convexity arguments, now applied to the map that gives the time spent by the asymmetric orbits  $C_l$  and  $C_r$  as functions of  $\tilde{\alpha}$ , allow us to conclude that those solution branches do not possess turning points.

Collecting this information graphically, we obtain the bifurcation diagram presented in Figure 8, where the bifurcation parameter is  $L$  and the bifurcation variable is the value

of the  $y$ -component of the solution at time  $t = -L$  (i.e. is the value of the  $y$ -component of the starting point of the orbit, which, of course, lies in the vertical line  $x = -\phi_p$ ).

Using the methods of Schaaf [10], it is possible to conclude that all solutions that do not arise in the pitchfork bifurcation at  $L^*$  are linearly unstable for the semiflow generated by (1.2)–(1.4).

### 3.4 Non-bifurcating solutions

We now finish the phase space analysis with a study of the non-bifurcating solutions to (2.2)–(2.3) that lie in the unbounded regions of the cylindrical phase space, i.e. those periodic solutions that exist above the homoclinic loop  $\gamma_h$ , or below  $\gamma_{-h}$ . As a consequence of this study, we then present the bifurcation diagram that sums up the analysis developed thus far. Let us start with the periodic solutions above the loop  $\gamma_h$ .

We already know, from the results in Section 3.2, that the branch of solutions leaving the bifurcation point  $L = L^*$  for  $L < L^*$  exists down to  $L = 0$ . By the analysis in that section and what was presented in Section 2 on the time map  $T_2$ , these solutions satisfy  $y(-L) \rightarrow +\infty$  as  $L \rightarrow 0$ . Remember that the  $x$ -component of these solutions is monotone increasing, so they are not periodic.

The periodic orbits above  $\gamma_h$  can be indexed by  $k$ , the number of times they fully circle the cylindrical phase space. An orbit of (2.2)–(2.3) that circles  $k$  times the phase space spends in its orbit a time given by  $2(kT_2(\beta_k, \frac{\pi}{2}) + T_2(\beta_k, \phi_p))$ , where  $\beta_k$  is the  $y$ -component of its intersection with the positive  $y$ -axis. Note that, from the phase space analysis, for each orbit, there is a one-to-one correspondence between the values of  $\beta_k$  and  $y(-L)$ , both converging to  $+\infty$  as  $L \rightarrow 0$ , and to the corresponding points in  $\gamma_h$  when  $L \rightarrow +\infty$ . From this and the results in Section 2, we conclude that, for each  $k \in \mathbb{N}$ , and each  $L > 0$ , there exists a unique solution to (2.2) circling exactly  $k$  times the cylindrical phase space, taking exactly  $2L$  units of time to do so, and its value of  $y(-L)$  converges to  $+\infty$  as  $L \rightarrow 0$  and to  $h_p$  (defined in the caption of Figure 8) when  $L \rightarrow +\infty$ . From the monotonicity properties of  $T_2$  studied in Section 2, we further conclude that  $y(-L)$  is monotonically decreasing with  $L$ .

By the symmetry properties of (2.2), exactly the same occurs with the orbits below  $\gamma_{-h}$ , the only difference being that, now, the time taken by a solution to (2.2)–(2.3) whose orbit circles  $k$  times the cylindrical phase space is  $2((k+1)T_2(\beta_k, \frac{\pi}{2}) - T_2(\beta_k, \phi_p))$ .

These results, together with those obtained in the Sections 3.1–3.3, can be joined together in order to draw the bifurcation diagram in Figure 9.

How all these solutions and bifurcation events are related to what happens as  $\phi_p \rightarrow 0^+$  is an interesting problem in its own right, but we do not address it here. Furthermore, a thorough understanding of the associated compact global attractor, along the lines of the work of, say, Fiedler and Rocha (see, for instance, [4] and related work) would require a knowledge of the Morse indices of the equilibria. It is, however, somewhat outside the scope of the present study.

## 4 Stability and monotonicity

We now recall the definitions introduced in Sections 1 and 2 for the re-scaled variables  $t$  and  $\zeta$  and for the parameter  $L$ , and re-scale the original time  $s \mapsto \tilde{s} := \frac{1}{2}s$ . Denoting

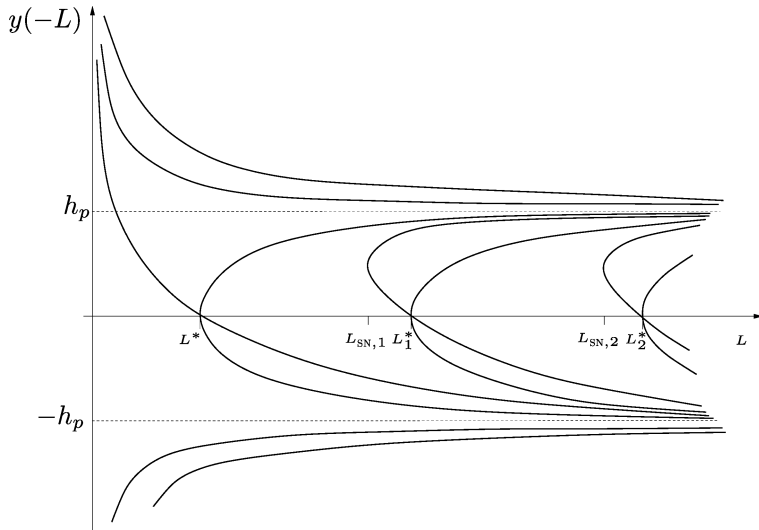


FIGURE 9. Part of the bifurcation diagram of (2.2)–(2.3) showing the pitchfork bifurcation points at  $L^*$ ,  $L_1^*$  and  $L_2^*$ , as well as four non-bifurcating solutions, two above  $\gamma_h$  and two below  $\gamma_{-h}$ .

again by  $\phi = \phi(\tilde{s}, t)$  the function  $\phi(s(\tilde{s}), \zeta(t))$  where  $\phi(s, \zeta)$  is a solution of (1.2)–(1.4), we can write the initial-boundary value problem (1.2)–(1.4) in the form,

$$\frac{\partial \phi}{\partial \tilde{s}} = \frac{\partial^2 \phi}{\partial t^2} + \sin 2\phi, \quad (\tilde{s}, t) \in \mathbb{R}^+ \times (-L, L), \quad (4.1)$$

$$\phi(\cdot, -L) = -\phi_p, \quad \phi(\cdot, L) = \phi_p, \quad (4.2)$$

$$\phi(0, \cdot) = \phi_0. \quad (4.3)$$

Note the equilibria of (4.1)–(4.3) are the solutions  $x(t)$  of (2.2)–(2.3).

Let us fix  $\phi_p \in (0, \pi/2)$ . Let  $L^*$  be given by (2.9). Denote by  $x^*(t)$  the monotone solution of (2.2)–(2.3) for  $L = L^*$ . Remembering Section 3.1,  $x^*(t)$  satisfies both Dirichlet and homogeneous Neumann boundary conditions. In this section, we show that there is a pitchfork bifurcation of  $\mathbb{Z}_2$ -symmetry breaking solutions from  $x^*(t)$ , which is thus concomitant with loss of monotonicity. By the principle of exchange of stability, this implies that the only stable solutions (more precisely, locally asymptotically stable for the semi-flow generated by (4.1)–(4.3), and hence also by (1.2)–(1.4)) are either monotone (for  $L \leq L^*$ , the symmetric solution) or have a unique extremum point (the non-symmetric solutions, for  $L > L^*$ ). The bifurcation that, as we show, occurs at  $L^*$  has to be a pitchfork bifurcation by the  $\mathbb{Z}_2$  symmetry of the equations, and it has to be a supercritical pitchfork bifurcation by the monotonicity results in Proposition 1. We have,

**Theorem 1** *There is a  $\mathbb{Z}_2$ -symmetry breaking bifurcation at  $L^*$  from the solution  $x^*(t)$  defined above. Furthermore, there cannot exist a bifurcation from a monotone solution  $\bar{x}(t)$  that does not satisfy the Neumann boundary condition.*

**Proof** Let the operator  $A_L$  with homogeneous Dirichlet boundary conditions on  $(-L, L)$  be defined by

$$A_L = \frac{d^2}{dt^2} + 2 \cos(2x(t; L)),$$

where  $x(t; L)$  is a solution of (2.2)–(2.3) for some fixed value of the parameter  $L$ . Since  $(x^*)'(\pm L^*) = 0$ , the function  $\psi(t) = (x^*)'(t)$  is a zero eigenfunction of  $A_L$ . Since the eigenvalue problem for this operator is a standard regular Sturm–Liouville problem with homogeneous Dirichlet boundary conditions, we know that all its eigenvalues are simple. Thus, by Krasnoselskii’s theorem [6],  $L^*$  is a bifurcation point.

To prove the second statement of the Theorem, let us proceed by contradiction. Suppose such a bifurcation occurs. Then, by the Krein–Rutman theorem [7], there is a function  $\psi(t) > 0$  satisfying homogeneous Dirichlet boundary conditions, such that

$$A_T \psi := \psi'' + 2 \cos(2\bar{x}(t))\psi = 0.$$

Furthermore,  $\psi'(-L) > 0$ ,  $\psi'(L) < 0$ , because otherwise, by the uniqueness theorem for linear ODEs,  $\psi(t)$  is identically zero. Now let  $\rho(t) = \bar{x}'(t)$ . Then

$$\rho'' + 2 \cos(2\bar{x}(t))\rho = 0,$$

and (since  $\bar{x}(t)$  is strictly monotone)  $\rho(\pm L) > 0$ . But then multiplying the equation satisfied by  $\psi$  by  $\rho$ , and vice versa, integrating over  $[-L, L]$  and subtracting, we have that

$$\psi'(L)\rho(L) - \psi'(-L)\rho(-L) = 0,$$

which is impossible, as this expression is necessarily negative. □

Finally, we have the following theorem (which again has been found numerically in [8, 9]):

**Theorem 2** *The map  $\phi_p \mapsto L^*$  is monotone increasing.*

**Proof** Fix  $\phi_p$  in  $(0, \frac{\pi}{2})$  and consider the critical solution  $x^*(t)$ . This function gives rise to a solution  $X^*(t)$  of (2.2) with homogeneous Dirichlet boundary conditions as follows:

$$X^*(t) = \begin{cases} x^*(t + L^*), & t \in [-L^*, 0) \\ -x^*(t - L^*), & t \in [0, L^*] \end{cases}.$$

Remembering that in Section 2 we denoted by  $\beta^* := \beta(\phi_p)$  the ordinate of the point of intersection of the critical solution with the  $y$ -axis, we immediately conclude, from a brief inspection of the phase portrait in Figure 3, that the map  $f_1 : \phi_p \mapsto \beta^*$  is monotone increasing. On the other hand, by a calculation as in Proposition 1, the (time) map  $f_2$  which measures the time it takes for a solution through the point  $(0, a)$ ,  $a \in [0, \sqrt{2})$ , to hit the point  $(0, -a)$  is monotone increasing. Furthermore,  $f_2(\beta^*) = 2L^*$ . Hence  $\frac{1}{2}f_2 \circ f_1$  is monotone increasing; but this is the map  $\phi_p \mapsto L^*$ , which concludes the proof. □



Defining

$$\lambda_c(\phi_p) := 8(L^*)^2, \tag{4.4}$$

we conclude, by (2.1) and the previous results, that  $\lambda_c(\phi_p)$  is the first bifurcation value of (1.2)–(1.4) and that the monotonicity, the symmetry and the stability properties of the bifurcating solutions are as stated in the Introduction.

### 5 Conclusions

We summarize our results and some consequences. The twist-Fréedericksz geometry (in-plane field perpendicular to planar-aligned director) is one of the three main Fréedericksz-transition geometries (the other two being the ‘bend’ and the ‘splay’ [3]). The instabilities associated with these systems are fundamental in the macroscopic equilibrium theory of liquid crystals and are of intrinsic interest. We have analysed the twist-Fréedericksz transition with pre-twist and some of the surprising features discovered numerically by Millar and McKay [8, 9]. In systems such as these, it is usually the case that altering the boundary conditions destroys the mirror symmetry and leads to an imperfect bifurcation and smeared-out transition. For the twist geometry, however, in the presence of antisymmetric pre-twist boundary conditions (equal absolute value and opposite signs on the opposing sides of the boundary), the system retains  $\mathbb{Z}_2$  symmetry and a symmetry-breaking pitchfork bifurcation, albeit at an elevated threshold.

The most distinguishing feature of the transition (with pre-twist) is the coincidence of the symmetry-breaking bifurcation with the loss of monotonicity of the ground-state solution (and simultaneous satisfaction of both Dirichlet and homogeneous Neumann boundary conditions  $\phi'(0) = \phi'(1) = 0$ ). A good framework within which to study this is the phase plane, where the problem coincides with that of a nonlinear pendulum. There, by analysing appropriate time maps, we have shown that the trajectory of the solution of the equilibrium boundary value problem at the bifurcation point must coincide with a segment of an orbit that begins and ends on the horizontal axis, where necessarily  $\phi' = 0$ .

From a practical point of view, this transition provides a potential way to measure experimentally the pre-twist of a twist cell with differently aligned anchoring conditions. In such an experiment, one would steadily increase or decrease the magnetic field strength to determine the critical threshold  $H_c$  of the onset of the instability. The relationship between  $H_c$  and  $\phi_p$  is monotone, hence invertible. It is given (in dimensionless terms) by (4.4), which can be written as

$$\lambda_c(\phi_p) = 8(L^*)^2 = 8(T(\phi_p))^2, \quad 0 \leq \phi_p < \frac{\pi}{2}. \tag{5.1}$$

Recalling (1.5), the parameter  $\lambda$  and the magnetic field strength  $H$  are related by

$$\lambda = \frac{\mu_0 \Delta \chi H^2 d^2}{K_2} \Leftrightarrow H = \frac{1}{d} \sqrt{\frac{K_2}{\mu_0 \Delta \chi}} \sqrt{\lambda}.$$

While an explicit formula for  $\phi_p$  in terms of  $\lambda_c$  or  $H_c$  cannot be given, formula (5.1) can easily be inverted, and Theorem 2 implies that  $\phi_p \mapsto \lambda_c(\phi_p)$  is monotone increasing for the full range of values of  $\phi_p \in (0, \pi/2)$ . For small values of the pre-twist angle  $\phi_p$ , the

fact that  $T(\alpha) = \frac{1}{\sqrt{2}}K(\sin^2 \alpha)$  allows one to obtain the approximation:

$$\lambda_c(\phi_p) \approx \pi^2 \left( 1 + \frac{1}{2}\phi_p^2 \right), \quad \text{when } \phi_p \approx 0,$$

which was found in [8] to give very good agreement with numerical results.

A final result worth noting concerns the characterization of the non-bifurcating periodic solutions in Section 3.4. In addition to allowing us to complete our phase-space analysis, these solutions are of some physical interest as well, for it is in these unbounded regions of the cylindrical phase space above  $\gamma_h$  and below  $\gamma_{-h}$  that one finds all ‘super-twisted’ solutions, that is, solutions with total twist across the cell greater than  $\pi$  radians. Super-twisted cells are used in display applications, although they are typically switched by electric (not magnetic) fields that are aligned perpendicular to (rather than parallel to) the film plane. STNs (Super-Twisted Nematic cells,  $\frac{3\pi}{2}$  radians total twist) are preferred to standard TNCs (Twisted Nematic Cells,  $\frac{\pi}{2}$  radians total twist) in some applications because of their shorter switching time. Our analysis readily guarantees existence and uniqueness of super-twisted solutions (both clockwise and counter-clockwise) of arbitrarily large total twist and for all field strengths. Of course, for given orientations of the director on the substrate boundaries, the solution with smallest total twist would have the least free energy.

### Acknowledgements

We thank Geoff McKay for allowing us to use the postscript file of Figure 1. F. P. da Costa and J. T. Pinto were partially supported by Fundação para a Ciência e a Tecnologia through Program POCI 2010/FEDER. E. C. Gartland, Jr. was partially supported by NSF grants DMS-0456221 and DMS-0608670.

### References

- [1] ABRAMOWITZ, M. & STEGUN, I. A. (editors) (1972) *Handbook of Mathematical Functions*, Dover, New York.
- [2] CHANDRASEKHAR, S. (1992) *Liquid Crystals*, 2nd ed., Cambridge University Press, Cambridge.
- [3] DA COSTA, F. P., GRINFELD, M., MOTTRAM, N. J. & PINTO, J. T. (2007) Uniqueness in the Freedericksz transition with weak anchoring (to appear in *J. Differ. Equ.*).
- [4] FIEDLER, B. & ROCHA, C. (1996) Heteroclinic orbits of semilinear parabolic equations. *J. Differ. Equ.* **125**, 239–281.
- [5] DE GENNES, P. G. & PROST, J. (1993) *The Physics of Liquid Crystals*, 2nd ed., Clarendon Press, Oxford.
- [6] KRASNOSELSKII, M. (1964) *Topological Methods in the Theory of Nonlinear Integral Equations*, MacMillan, New York.
- [7] KREIN, M. & RUTMAN, M. (1962) Linear operators leaving invariant a cone in banach space (Engl. Transl.). *Am. Math. Soc. Transl., Ser. 1*, **10**, 199–325.
- [8] MILLAR, H. (2007) *Mathematical Modelling of Nematic and Smectic Liquid Crystals*, PhD thesis, University of Strathclyde, Glasgow.
- [9] MILLAR, H. & MCKAY, G. (2005) Director orientation of a twisted nematic under the influence of an in-plane magnetic field. *Mol. Cryst. Liq. Cryst.* **435**, 277/[937]–286/[946].

- [10] SCHAAF, R. (1990) *Global Solution Branches of Two Point Boundary Value Problems*, Lecture Notes in Mathematics, Vol. 1458. Springer-Verlag, Berlin.
- [11] SMOLLER, J. & WASSERMAN, A. (1981) Global bifurcation of steady-state solutions. *J. Differ. Equ.* **39**, 269–290.
- [12] STEWART, I. W. (2004) The Static and Dynamic Continuum Theory of Liquid Crystals. *The Liquid Crystals Book Series, Vol. 2*, Taylor & Francis, London.
- [13] VIRGA, E. G. (1994) Variational Theories for Liquid Crystals. *Applied Mathematics and Mathematical Computation, Vol. 8*, Chapman & Hall, London.